NASA / TM—2000-210240 AIAA–2000–2348

Analysis of the Laser Propelled Lightcraft Vehicle

Douglas Feikema
Glenn Research Center, Cleveland, Ohio

June 2000

The NASA STI Program Office . . . in Profile

Since its founding, NASA has been dedicated to the advancement of aeronautics and space science. The NASA Scientific and Technical Information (STI) Program Office plays a key part in helping NASA maintain this important role.

The NASA STI Program Office is operated by Langley Research Center, the Lead Center for NASA's scientific and technical information. The NASA STI Program Office provides access to the NASA STI Database, the largest collection of aeronautical and space science STI in the world. The Program Office is also NASA's institutional mechanism for disseminating the results of its research and development activities. These results are published by NASA in the NASA STI Report Series, which includes the following report types:

- TECHNICAL PUBLICATION. Reports of completed research or a major significant phase of research that present the results of NASA programs and include extensive data or theoretical analysis. Includes compilations of significant scientific and technical data and information deemed to be of continuing reference value. NASA's counterpart of peer-reviewed formal professional papers but has less stringent limitations on manuscript length and extent of graphic presentations.

- TECHNICAL MEMORANDUM. Scientific and technical findings that are preliminary or of specialized interest, e.g., quick release reports, working papers, and bibliographies that contain minimal annotation. Does not contain extensive analysis.

- CONTRACTOR REPORT. Scientific and technical findings by NASA-sponsored contractors and grantees.

- CONFERENCE PUBLICATION. Collected papers from scientific and technical conferences, symposia, seminars, or other meetings sponsored or cosponsored by NASA.

- SPECIAL PUBLICATION. Scientific, technical, or historical information from NASA programs, projects, and missions, often concerned with subjects having substantial public interest.

- TECHNICAL TRANSLATION. English-language translations of foreign scientific and technical material pertinent to NASA's mission.

Specialized services that complement the STI Program Office's diverse offerings include creating custom thesauri, building customized data bases, organizing and publishing research results . . . even providing videos.

For more information about the NASA STI Program Office, see the following:

- Access the NASA STI Program Home Page at ***http://www.sti.nasa.gov***

- E-mail your question via the Internet to help@sti.nasa.gov

- Fax your question to the NASA Access Help Desk at (301) 621-0134

- Telephone the NASA Access Help Desk at (301) 621-0390

- Write to:
  NASA Access Help Desk
  NASA Center for AeroSpace Information
  7121 Standard Drive
  Hanover, MD 21076

NASA / TM—2000-210240 AIAA–2000–2348

Analysis of the Laser Propelled Lightcraft Vehicle

Douglas Feikema
Glenn Research Center, Cleveland, Ohio

Prepared for the
31st Plasmadynamics and Lasers Conference
sponsored by the American Institute of Aeronautics and Astronautics
Denver, Colorado, June 19–22, 2000

National Aeronautics and
Space Administration

Glenn Research Center

June 2000

Acknowledgments

The author gratefully acknowledges the financial support of NASA MSFC and the American Society of Engineering Education (ASEE) under the 1998 and 1999 summer faculty fellowship program. The author also gratefully acknowledges the assistance of Mr. Kevin Buch and Mr. Sandy Kirchendal during the summer of 1999.

Available from

NASA Center for Aerospace Information
7121 Standard Drive
Hanover, MD 21076
Price Code: A03

National Technical Information Service
5285 Port Royal Road
Springfield, VA 22100
Price Code: A03

AIAA–2000–2348

ANALYSIS OF THE LASER PROPELLED LIGHTCRAFT VEHICLE

Douglas Feikema
National Aeronautics and Space Administration
Glenn Research Center
Cleveland, Ohio 44135

ABSTRACT

Advanced propulsion research and technology require launch and space flight technologies, which can drastically reduce mission costs. Laser propulsion is a concept in which energy of a thrust producing reaction mass is supplied via beamed energy from an off-board power source. A variety of laser/beamed energy concepts were theoretically and experimentally investigated since the early 1970's. During the 1980's the Strategic Defense Initiative (SDI) research lead to the invention of the Laser Lightcraft concept. Based upon the Laser Lightcraft concept, the U.S. Air Force and NASA have jointly set out to develop technologies required for launching small payloads into Low Earth Orbit (LEO) for a cost of $1.0M or $1000/lb to $100/lb. The near term objectives are to demonstrate technologies and capabilities essential for a future earth to orbit launch capability. Laser propulsion offers the advantages of both high thrust and good specific impulse, I_{sp}, in excess of 1000 s. Other advantages are the simplicity and reliability of the engine because of few moving parts, simpler propellant feed system, and high specific impulse. Major limitations of this approach are the laser power available, absorption and distortion of the pulsed laser beam through the atmosphere, and coupling laser power into thrust throughout the flight envelope. The objective of this paper is to assist efforts towards optimizing the performance of the laser engine. In order to accomplish this goal (1) defocusing of the primary optic was investigated using optical ray tracing and (2), time dependent calculations were conducted of the optically induced blast wave to predict pressure and temperature in the vicinity of the cowl. Defocusing of the primary parabolic reflector causes blurring and reduction in the intensity of the laser ignition site on the cowl. However, because of the caustic effect of ray-tracing optics the laser radiation still forms a well-defined ignition line on the cowl. The blast wave calculations show reasonable agreement with previously published calculations and recent detailed CFD computations.

NOMENCLATURE

C	average plasma velocity
D*	injector diameter
E	laser energy deposited
h	enthalpy
I	laser intensity
I_{SP}	specific impulse
L	plasma length
M	molecular weight
P	gas pressure
q	heat addition from laser
r	blast wave radius
R_U	universal gas constant
T	gas temperature
t	time
u*	sonic gas injection velocity
V	blast wave velocity
Z	gas compressibility factor

Greek

ρ	gas density
η	percentage of laser energy absorbed
γ	ratio of specific heats

Subscripts

CJ	Chapman-Jouget Condition
LSD	laser supported detonation
o	initial or ambient state
p	laser pulse
REF	reference condition
2D	two-dimensional

INTRODUCTION

Advanced propulsion concepts for the 21st century include the use of beamed energy such as a ground based laser to provide thrust to a vehicle propelled by a laser-induced blast wave.[1,2] Jointly, the U.S. Air Force and NASA have set out to develop technologies and concepts required for launching small payloads into Low Earth Orbit (LEO) for a total cost of $1.5M or $1000/lb to $100/lb. This concept is shown schematically in Fig. 1. Among the technology options available, one potential high pay off approach is using a high power pulsed laser as an off board energy source.[3] Laser propulsion offers the advantages of both high thrust and theoretically infinite specific impulse, I_{sp}, at altitudes less 20 km during the first stage and high thrust and specific impulse in excess of 1000 s during the second stage above 20 km. Other advantages are the simplicity and reliability of the engine because of few moving parts, simpler propellant feed system, and high specific impulse. Major limitations of this approach are the laser power available,[4] absorption and distortion of the pulsed laser beam through the atmosphere,[5] and coupling laser power into thrust throughout the flight envelope.[6]

Successful operation of a pulsejet engine relies on synchronous interplay of complex transient phenomena and the introduction of new vehicle design concepts, which integrate the total mission requirements.[6-9,19] The mission requirements include blast wave formation and propagation, pulsed laser heating, inlet air replenishment in air-breathing mode, first stage, and propellant injection in rocket mode, second stage.

The concept of Laser Propulsion originates to at least 1972 and is accredited to Kantrowitz.[3] During the 1960's after the invention of the laser, scientists investigated the basic phenomenon of laser-induced breakdown of gases and plasma ignition which forms the fundamental basis of pulsed laser propulsion.[12-15] During the remainder of the 1970's, much attention was directed towards conceptual design and basic research of using beamed energy from a ground based laser to assess the possibility and feasibility of laser energy for rocket propulsion.[16] Several of these studies involved laboratory scale experimentation for proof of concept. One of the most promising of these concepts at this time appears to be the repetitively pulsed (RP) laser concept.[1,10-11] Typically, a laser pulse is fired into the rear of a parabolic reflecting engine/nozzle where the high-intensity radiation is sufficient to cause an electrical breakdown of a small propellant volume creating a high temperature, rapidly expanding plasma. This plasma, which closely resembles a supersonic blast wave, rapidly exits a supersonic nozzle to create thrust.

Two methods for obtaining thrust using the RP concept from laser radiation have been considered. The first involves rapid vaporization of a solid propellant with a first pulse followed by a second pulse, which forms plasma at the surface, and the formation of a laser supported detonation (LSD) wave. A second approach involves focusing the laser intensity into a gas near a solid surface in order to break down the gas and induce a detonation wave transferring momentum to the surface. Previous research has shown that ablation and pitting of the surfaces occur which can strongly reduce the efficiency of the laser absorption process. Raizer[12] (1977) noted for high temperature air where $I = 10^5$ MW/cm^2, $\rho_o = 1.3\times10^{-3}$ g/cm^2, and $\gamma = 1.33$ that $V_{LSD} = 133$ km/s and $T_{equilibrium} = 910{,}000$ K. These values were in reasonable agreement with experiment, $V_{LSD} = 110$ km/s and T = 700,000 K. Therefore, future advances in pulsed detonation laser propulsion will require mitigating the adverse effects of material degradation in the regions of intense laser radiation, which induces high plasma temperatures [12] in the vicinity of the surface.

Pirri[8] et al. (1974) reported on experiments utilizing a solid and a gas propellant. They concluded that the best way to achieve a high specific impulse is to add laser energy directly to gas rather than to first vaporize a solid propellant. In order to further improve performance of the laser engine, a mixture of low molecular weight propellant and a small percentage of an easily ionizable seed (i.e., H_2 or He plus Li or Cs) as a seed to the gaseous propellant may provide improvements. Such improvements would enable shorter duration laser pulses of higher power, which would enable high thrust times and higher specific impulse.

In the past several studies have been conducted to investigate various effects which include threshold breakdown laser intensities above various surfaces in air, the effect of air pressure and density on threshold energies, and the vaporization of various solid materials. Maher[13] et al. (1973) reported that the ignition thresholds for laser supported detonation waves for selected materials were determined in air at one atmosphere pressure. The type of solid reflecting material has an important effect. For example, for aluminum the measured threshold laser intensity is 59 J/cm^2 and fused silica it is 310 J/cm^2. Therefore, careful selection of the solid reflecting surface requires careful consideration.

Hettche[15] et al. concluded that the impulse coupled to the solid surface is controlled by the interaction between the laser energy and air breakdown products at the surface. They also noted from the pressure measurements generated by laser fluxes of 1×10^8 to 3×10^8 W/cm^2 the peak pressure generated varied from ~20 to 220 atmospheres. However, the measured pressure relaxes rapidly behind the expanding plasma front. Coupling of the pressure to the target surface after the initial reaction is dependent on the complex interaction between the opacity of the dispersing plasma and the incident beam intensity.

Currently, laser propelled Lightcraft vehicles[10,11] are being successfully flown in a series of experiments conducted at the High Energy Laser Systems Test Facility (HELSTF), White Sands Missile Range, New Mexico. The axisymmetric Lightcraft vehicles are propelled by airbreathing, pulsed-detonation engines (PDE) with an infinite specific impulse. Spin-stabilized, free-flight launches have been conducted and were limited to altitudes approaching 30 m. High speed Schlieren and shadow-graph pictures have shown that the laser-induced shock wave wraps around the outer perimeter of the engine's shroud. Also, testing has shown the shroud or cowl structure fails after 100 laser firings into the thrust cavity.

The grand vision[19] is to integrate the Lightcraft concept into an earth-to-orbit vehicle. This concept includes launching a 2-meter diameter Lightcraft vehicle with initial mass of 100 kg into low earth orbit using a 100 MW laser. The Lightcraft vehicle operates in air-breathing mode to about 20 km, then transitions into rocket mode using an onboard inert propellant to a vertical ascent of 100 km. At 100 km the vehicle turns over and acceleration down range occurs at 5 to 6 degrees from horizontal. Burnout would occur at ~1000 km after ~15 mins from launch with an estimated payload of 150 kg in orbit.

A cost estimate for a smaller system,[4] however, using a 20 MW laser, 20 kg orbital payload, and 150 kg of propellant would cost $500M to establish the laser facility, telescope, adaptive optics, tracking, power generating plant and the structural facility. The 20 MW – 20 kg system was noted to be the smallest size that would be cost effective. Larger systems gain linearly in payload size versus laser power. It is perhaps best to begin development of a lower power, low payload system first in order to develop and demonstrate technology to provide proof of concept before a (i.e., 1 GW – 1000 kg) system is implemented.

THEORETICAL DESCRIPTION OF THE LASER SUPPORTED DETONATION (LSD) WAVE

The basic phenomenon occurring inside the nozzle is the ionization of gas, plasma ignition, and blast wave propagation.[12] During the 1960's scientists demonstrated that a focused laser beam from a high power laser beam in stagnant gas produced electrical breakdown and the propagation of a blast or detonation wave.[13-15] When the intense laser radiation was focused next to a solid surface, impulse and momentum exchange was observed and quantified.

The inverse bremsstrahlung effect (IB)[12,17] is the prime process assisting to achieve the very high plasma temperatures (10^4 to 10^5 K) necessary for laser engine operation and creation of high thrust. Initial ionization of the plasma takes place in the gas as a result of focusing the laser beam to higher laser intensities than the threshold value, which generates free electrons. When the plasma is ignited its unobstructed length[18] can be estimated by:

$$L = 2V_{LSD}t_p \tag{1}$$

L is the initial length of the plasma, V_{LSD} is the plasma detonation velocity, and t_p is the laser pulse duration. In this plasma zone the laser beam energy is absorbed into the gas and L is proportional to the electron mean free path. The ionization process is faster and therefore shorter than a single laser pulse. During the remainder of the laser pulse free electrons are accelerated until the laser pulse ends. The gas temperature rises, the plasma length increases, which leads to expansion of the hot plasma region. After the laser pulse terminates, a blast wave front exists because of the high energy absorbed in the plasma, causing further ionization of the cold gas layers. Raizer[17] noted that the majority of the laser energy is already absorbed into the plasma rather than in the gas, because the plasma ignited about 9 ns after firing the laser whereas the laser pulse duration was 30 ns. Because L increases with temperature and time, the location where high-speed electrons come into contact with the cold gas front is eventually shifted away from the focal point. When the propagation distance of the plasma exceeds the outer boundaries of the cold gas in the nozzle cavity, the wave front simply evaporates into the vacuum outside the gas boundaries.

The initial absorption wave or Laser Supported Detonation (LSD) wave velocity[12] is:

$$V_{LSD} = \left[2(\gamma^2 - 1)\frac{I}{\rho_o} \right]^{1/3} \tag{2}$$

where the maximum heat absorbed or energy release by the wave is:

$$q = I/\rho_o V_{LSD} \tag{3}$$

and I is the laser intensity (W/m^2), ρ_o is the initial gas density, and γ is the ratio of specific heats. The conservation of mass and energy applied across the initial LSD wave can be combined to give:[17]

$$h_0 + \frac{V_{LSD}^2}{2} + \eta q = h + \left[\frac{\rho_0}{\rho} \right]^2 \frac{V_{LSD}^2}{2} \tag{4}$$

where h is the enthalpy and η is the percentage of laser energy absorbed into the gas. Reilly et. al.[21] note that this conversion efficiency is typically 80 to 90 percent. The pressure generated directly behind the Laser Supported Detonation (LSD) wave front corresponds to the upper Chapman-Jouget point[17] and is given by:

$$P_{CJ} = \frac{\rho_0 V_{LSD}^2}{(\gamma+1)} \tag{5}$$

By applying the method of characteristics combined with Raizer's equations, the blast wave expansion process can be described. For the case when a flat surface or plate is placed at the focal point normal to the axis of the laser beam the maximum pressure on the surface of the plate is given by:[19]

$$P_{LSD} = \left[\frac{\gamma+1}{2\gamma}\right]^{\frac{2\gamma}{\gamma-1}} \frac{\rho_0 V_{LSD}^2}{(\gamma+1)} \tag{6}$$

The self-similar solutions for the set of differential equations for axisymmetric and isentropic conditions were analyzed by Sedov.[20] These solutions are used to determine flow and thermodynamic variables scaled to a reference point corresponding to a cylindrical blast wave when the blast wave has evolved into a cylindrical shape which corresponds to plasma ignition adjacent to a flat plate. The unpowered Sedov scaling law's used for the present set of conditions for pressure behind the blast wave and the radius of the wave are:

$$P/P_{REF} = \left(t/t_{REF}\right)^{-1};\ r/r_{REF} = \left(t/t_{REF}\right)^{1/2} \tag{7}$$

The reference conditions[19] P_{REF} is P_{LSD}, t_{REF} is t_{2D}[21] or the time for the blast wave to evolve into a completely cylindrical expansion, and r_{REF} corresponds to the radius of the wave when wave can be considered completely cylindrical, r_{LSD}. Shortly after the laser pulse is completed, a rarefaction wave moves in from the edges of the blast wave front, according to the method of characteristics this wave travels at an average plasma velocity of C_{LSD}

$$C_{LSD} = \frac{V_{LSD}}{2} = \sqrt{\frac{\gamma P}{\rho}} \tag{8}$$

When this rarefaction fan first arrives at the centerline of the surface the blast wave geometry is considered to be completely cylindrical such that:[21]

$$t_{2D} = \frac{r_{LSD}}{C_{LSD}} \tag{9}$$

A simplistic thermodynamic relation for the plasma expansion is assumed using an equation of state incorporating the compressibility factor, Z, such that:[19]

$$T = \frac{C_{LSD}^2}{\gamma Z R_u/M} \tag{10}$$

where M is the gas molecular weight.

RESULTS AND DISCUSSION

Design Approaches Suggested by Specific Impulse

Simmons and Pirri[6] derived an analytic expression for the specific impulse, I_{sp}, of a repetitively pulsed laser ignited thruster. The payload mass can be maximized by maximizing the specific impulse:

$$I_{sp} \approx \frac{(u^*)^{1/2}(E)^{1/2}}{M^{1/4}(t_p - t_s)^{1/2} D^*} \tag{11}$$

where u* is the gas sonic injection velocity in the thrust cavity, E is the total laser energy deposited, D* is the nozzle throat diameter, t_p is the time between pulses, M is the propellant molecular weight, and t_s is the ignition time of the blast wave. As noted by this expression the payload mass fraction can be improved by (1) Pulsing the laser at a high rate preferably close to the same rate as the ignition time (i.e. < 1 μsec), (2) Increasing the total laser energy deposited, (3) Using low molecular weight propellants, (4) Injecting hot gas instead of a cold gas during the second stage since u* is higher, and (5) Injecting propellant through a small throat diameter. They also noted an important difference between this expression and that of a chemical rocket. The specific impulse for a pulsed laser system favors a low molecular weight propellant but not by as large a margin as in a chemical rocket where $I_{sp} \sim (M)^{-1/2}$. Therefore, the possibility of using heavier propellants than in chemical systems opens the door for some revolutionary new opportunities.

Optical Ray Tracing: Effect of Off-Axis Defocusing of Primary Optic

One aspect in assessing the performance of the lightcraft pulsed laser engine involves studying the effects of defocusing the laser radiation caused by misalignment of the laser beam with respect to the primary optic. These effects will affect flight stability and performance of the laser engine and are more likely to occur as the distance between the vehicle and the ground based laser increase because of the atmospheric effects on the laser radiation.[5]

An optical ray-tracing program called code V developed by Optical Research Associates, Inc. was used to analyze the effectiveness of the lightcraft parabolic reflector to focus laser light at a laser wavelength of 10.6 μm with off axis focusing. Figure 2 shows a cross section of one optical set-up under perfectly focused conditions. The optical system consists of (1) the point source at 10 miles behind or to the left of the lightcraft, (2) the aperture or diameter of the vehicle, 4.4 in. (3) the parabolic reflector with a focal distance of ~0.5 in. and (4) the cowl or image surface. Figures 2 and 3 show the optical system perfectly focused with traced rays in two and three-dimensional perspectives respectively. Only rays of

light originating from the source, which enter through the aperture or ring in Fig. 3, are reflected off the 100 percent reflective parabolic surface of revolution. All rays terminate on the image plane or cowl, which is shown in Fig. 3 as a bent, rectangular strip wrapped around the axisymmetric parabolic reflector. In this case the laser beam and the lightcraft are perfectly aligned. The parabolic reflector is similar in size and shape to the actual flight test vehicle recently conducted.[10,11] Figure 4 shows the parabola used to construct the primary optic surface for the optical ray-tracing program results reported here. The equation for this relation in units of inches is given by:

$$z(y) = 1.9504y - 0.4564y^2 \qquad (12)$$

The intensity of laser radiation on the top half perimeter of the cowl, 180°, is shown in Fig. 5 in arbitrary units. This cowl surface has been flattened out and the intensity of the laser radiation in arbitrary units has been plotted as a function of height on this surface. For the case of perfect alignment, the intensity is constant along the hemisphere or length of the cowl and a well-defined ignition line is observed. Figures 6 and 7 show the effect of rotating the lightcraft 5 degrees about the x-axis. The intensity of the focused laser energy on the cowl is shown in Fig. 7. The intensity of the radiation is a factor of 4.5 less than the perfectly focused case and nearly constant along the ignition line. It is observed, however, that the ignition line is now curved rather than being straight. Figure 8 shows the effect of rotating the lightcraft 5 degrees about the y-axis. The peak intensity in the center, which corresponds to the top of the cowl in Fig. 3, is reduced by a factor of 1.4 from the intensity level shown in Fig. 5. Significant blurring is observed with a high intensity on the top of the cowl and a line of decreasing intensity moving in either direction. Figure 9 shows the effect of rotating the lightcraft both 5 degrees about the x-axis and the y-axis. The intensity is blurred somewhat and is reduced in magnitude by a factor of 4.8. The spatial deviation of the focused laser intensity is observed to have a 0.5-in. variation in the y-axis and a well-defined ignition line is observed. This effect is known as the caustic effect in ray tracing optics whereby the rays tend to pile up onto a local region on the image plane. This is a positive observation of this study, namely that a well-defined ignition line of focused laser radiation is observed even when the primary optic is defocused. This implies that laser ignition will still occur under defocusing conditions but since the laser intensity varies along the perimeter of the cowl, the local thermodynamic conditions will also vary along the perimeter. This will induce multidimensional effects associated with the gas expansion process.

Blast Wave Calculations of the Expanding Plasma

An analysis and computation using MATHCAD and the NASA Glenn Chemical Equilibrium Code, CEA, 1999 were used to determine pressure and temperatures histories in the vicinity of the cowl. This analysis is described in detail in Refs. 19, 20, and 21 and the preceding section. In the calculation reported herein the following parameters were used in the model: $\gamma = 1.2$, $\rho_0 = 1.2$ kg/m^3, M = 28.97, Compressibility factor Z = 2.1, Laser pulse duration = 1×10^{-6} sec, size of plasma at end of pulse $|r_{LSD}$ = 5 mm, focused laser intensity I = 5×10^{11} Watts/m^2. Prior to the beginning of the laser pulse the air was assumed to be at room temperature and pressure. The surface pressure history on the cowl in the region of the focused laser radiation is shown in Fig. 10. The peak surface pressure builds up during the laser pulse to a peak pressure of about 250 atmospheres. The pressure decays very rapidly at t^{-1} as the plasma expands, however, and reaches atmospheric pressure after 350 μs or 250 nondimensional time units. The blast wave travels a distance of 7.9 cm when the blast wave has completely expanded.

In order to more accurately predict the initial state of the plasma and the temperature and composition of the gas, the NASA Glenn CEA code, 1999, was utilized. The maximum heat absorbed by the gas due to the laser flux is given by Eq. (3) to be 58.7 MJ/kg. Initially the peak pressure directly behind the wave as predicted by Eq. (5) is 271.8 ATM. Next, a T-P calculation using the NASA CEA 1999 code with a pressure of 271.8 ATM and an assigned temperature was completed for atmospheric air. The temperature and composition of the gas were determined by iteratively solving Eq. (4) with $\eta = 0.86$ and the NASA CEA code. A temperature of 17,400 K and pressure of 271.8 ATM gave good agreement between the computed enthalpies (7.0×10^7 J/kg) using Eq. (4) and the NASA CEA code assuming 86 percent of the laser energy is absorbed by the gas. The mole fractions of the highly ionized and dissociated gas as computed by the code are shown in table I.

In order to model the temperature decay of the expanding plasma a simple thermodynamic model is used to predict the gas temperature using Eq. (10). For a compressibility factor of Z = 2.1, M = 28.97, and $\gamma = 1.2$ a temperature of 17,400 K is computed. Figure 11 shows the gas temperature decay (t^{-1}) behind the blast wave for a laser intensity of 5×10^{11} W/m^2. Initially the temperature in the vicinity of the focused laser beam reaches a maximum of 17,400 Kelvin. The temperature is observed to decay rapidly to about 1800 Kelvin in 10 t_{2D} or 14 μs after the laser pulse.

Figure 12 shows the radius of the cylindrically propagating LSD Wave from initiation of the wave at t_{2D} of 1.41×10^{-6} seconds from a radius of 5 mm to a

final radius of 79 mm at 3.5×10^{-4} seconds at which point in time the blast wave has dissipated to one atmosphere of pressure. Figure 13 shows the blast wave velocity decay from initially 7100 m/s corresponding to a Mach number of 20. The wave velocity is observed to decay rapidly at $t^{-1/2}$. Figure 14 shows the effect of ambient gas density or altitude on the peak gas pressure for the conditions described above for a laser intensity of 5×10^{11} W/m^2. At an altitude of 20 km where the density of the air is ~0.01 kg/m^3 the peak surface pressure on the cowl has decreased from 250 ATM at sea level to 50 ATM at 20 km.

Since the focused laser intensity is such an important parameter in generating thrust and heating of the gas, the effect of laser intensity on the peak surface pressure and the peak equilibrium gas temperature is shown in Figs. 15 and 16. In Fig. 15 it is shown that the peak pressure can theoretically attain 10,000 ATM at 1×10^{14} W/m^2. Also, from Fig. 16 the theoretical peak gas temperatures approaches 10^6 °K when the laser intensity is 2×10^{14} W/m^2.

CONCLUSION

1. Defocusing of the primary parabolic reflector causes blurring and reduction in the intensity of the laser radiation at the ignition site on the cowl. However, because of the caustic effect of ray-tracing optics the laser radiation still forms a well-defined ignition line on the cowl. Under off axis focusing of 5°, the ignition line becomes curved and reduced in intensity by up to an order of magnitude in intensity.
2. The blast wave calculations show reasonable agreement with the values given in Ref. 19 and recent CFD calculations.[22] The pressure and temperature decay rapidly and the decay process is completed in 350 μs. The effected radius measured from the ignition site is 7.9 cm.

REFERENCES

1. Glumb, R.J. and Krier, H.," Concepts and Status of Laser-Supported Rocket Propulsion", *J. Spacecraft*, Vol. 21, No. 1, pp. 70–79, 1984.
2. Birkan, M.A.," Laser Propulsion: Research Status and Needs", *Journal of Propulsion and Power*, Vol. 8, No. 2, pp. 354–360, March–April 1992.
3. Kantrowitz, A.," Propulsion to Orbit by Ground Based Lasers", *Astronautics and Aeronautics*, Vol. 10, No. 5, pp. 74–76, May 1972.
4. Kare, J.T.," Pulsed Laser Propulsion for Low Cost, High Volume Launch to Orbit", *Space Power Journal*, Vol. 9, No. 1, pp. 6775, 1990.
5. Volkovitsky, O.A., Sedunov, Y.S., and Semenov, L.P., *Propagation of Intensive Laser Radiation in Clouds*, American Institute of Aeronautics and Astronautics, 1992.
6. Simmons, G.A. and Pirri, A.N.," The Fluid Mechanics of Pulsed Laser Propulsion", *AIAA Journal*, Vol. 15, No. 6, pp. 835–842, June 1977.
7. Nebolsine, P.E., Pirri, A.N. Goela, J.S., and Simmons, G.A.," Pulsed Laser Propulsion", *AIAA Journal*, Vol. 19, No. 1, pp. 127–128, Jan. 1981.
8. Pirri, A.N., Monsler, M.J., and Nebolsine, P.E.," Propulsion by Absorption of Laser Radiation", *AIAA Journal*, Vol. 12, No. 9, pp. 1254–1261, Sept. 1974.
9. Pirri, A.N.," Analytic Solutions for Laser-Supported Combustion Wave Ignition above Surfaces", *AIAA Journal*, Vol. 15, No. 1, pp. 83–91, Jan. 1977.
10. Mead Jr., F.B., Myrabo, L.K., and Messitt, D.G.,"Flight and Ground Tests of a Laser-Boosted Vehicle, 34th AIAA/ASME/SAE/ASEE Joint Propulsion Conference and Exhibit, Cleveland, OH, *AIAA 98–3735*, July 13–15, 1998.
11. Myrabo, L.N. and Messitt, D.G., and Mead Jr., F.B.," Ground and Flight Tests of a Laser Propelled Vehicle", 36th Aerospace Sciences Meeting and Exhibit, Reno, Nevada, *AIAA 98–1001*, Jan. 12–15, 1998.
12. Raizer, I.P., *Laser-Induced Discharge Phenomena*, Plenum Publishing Corporation, New York, NY, pp. 189–268, 1977.
13. Maher, W.E., Hall, R.B., and Johnson, R.R.," Experimental Study of Ignition and Propagation of LSD Waves", *Journal of Applied Physics*, Vol. 45, pp. 2138–2145, May 1974.
14. Pirri, A.N., Schlier, R., and Northam, D.," Momentum Transfer and Plasma Formation above a Surface with a High-Power CO_2 Laser", *Applied Physics Letters*, pp. 79–81, August 1972.
15. Hettche, L.R., Schriempf, J.T., and Stegman, R.L.,"Impulse Reaction Resulting from the in-air Irradiation of Aluminum by a Pulsed CO_2 Laser", *J. Appl. Physics*, Vol. 44, No. 9, pp. 4079–4085, Sept. 1973.
16. Caveny, L.H., Orbit Raising and Maneuvering Propulsion: Research Status and Needs, Vol. 89, *Progress in Astronautics and Aeronautics*, AIAA, New York, NY, 1984.
17. Raizer, I.P.," Breakdown and Heating of Gases Under the Influence of a Laser Beam", *Soviet Physics Uspekhi*, Vol. 8, No.5, pp. 650–673, March–April 1966.
18. Brandstein, A. and Levy, Y.," Laser Propulsion System for Space Vehicles", *Journal of Propulsion and Power*, Vol. 14, No. 2, pp. 261–269, March–April 1998.

19. Myrabo, L.N., "Transatmospheric Laser Propulsion: Lightcraft Technology Demonstrator", Final Technical Report, SDIO Laser Propulsion Program, Contract No. 2073803, pp. 117–142, 1989.
20. Sedov, L.L., *Similarity and Dimensional Methods in Mechanics*, Fourth Russian Ed., Academic Press, New York, NY, 1959
21. Reilly, J.P., Ballantyne, A., Woodroffe, J.A., "Modeling of Momentum Transfer to a Surface by Laser-Supported Absorption Waves," *AIAA Journal*, Vol. 17, No. 10, p. 1098–1105, 1979.
22. Personal Communication.

TABLE 1—Initial State of the Laser Ignited Air Plasma as Computed by NASA CEA, 1999, Equilibrium Air Mole Fractions at 271.8 ATM and 17,400 K.

*e-	1.0830-1	*N+	9.1863-2
*Ar	3.3503-3	*N-	7.4395-4
*Ar+	8.5684-4	NCO	3.782-11
*C	1.0079-4	*NO	3.6288-4
*C+	4.1572-5	*NO+	1.8947-4
*C-	1.8139-7	NO2	1.0435-8
*CN	4.5023-7	NO2-	1.307-11
*CN+	1.0521-7	NO3	1.380-14
CN-	7.833-10	*N2	1.5659-3
CNN	4.311-11	*N2+	5.6956-4
*CO	1.5655-7	N2-	2.1197-6
*CO+	4.9732-8	NCN	9.153-11
*CO2	8.008-12	N2O	2.7163-8
*CO2+	6.324-12	N2O+	4.1142-8
*C2	3.579-11	N3	4.7608-8
*C2+	2.597-11	*O	1.7189-1
C2-	1.130-13	*O+	1.5759-2
CCN	2.694-14	*O-	2.4471-4
CNC	3.885-14	*O2	1.5923-5
C2O	1.534-14	*O2+	8.6215-6
*N	6.0414-1	O2-	3.8408-8
		O3	4.5254-9

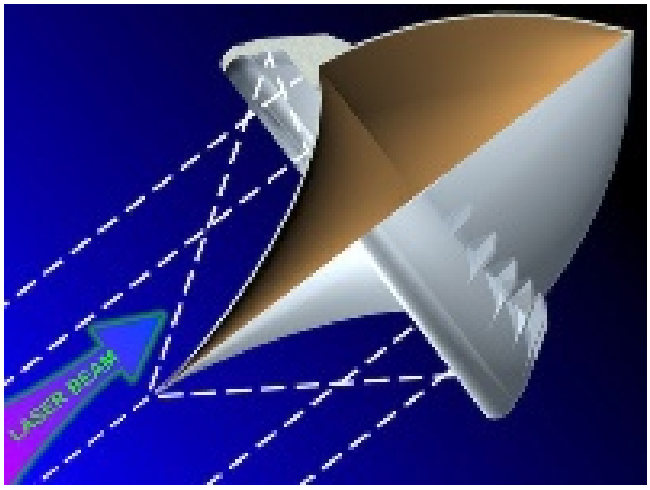

Figure 1.—The Laser Lightcraft Vehicle Propulsion Concept.

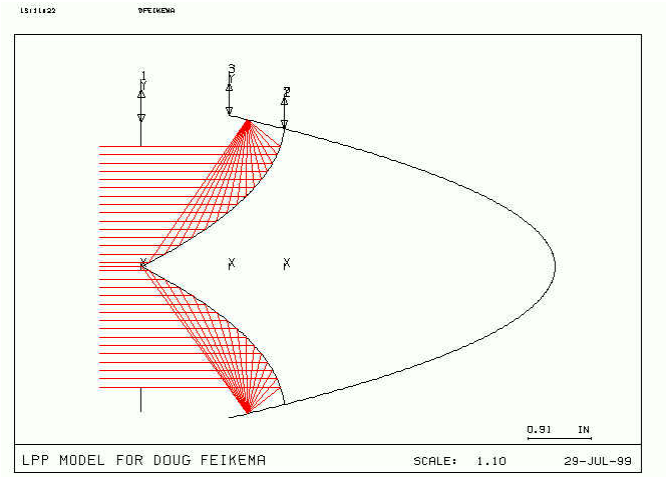

Figure 2.—Cross Sectional view of one Code V Optical System of Lightcraft Parabolic Reflector showing Ray Tracing for a perfectly focused laser beam.

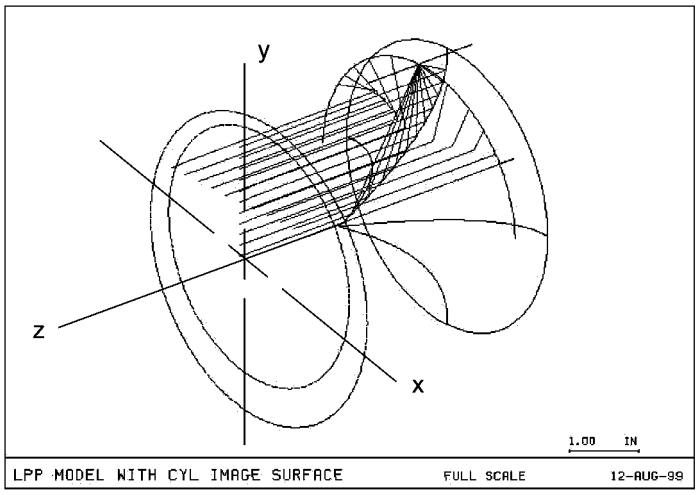

Figure 3.—Code V Optical System of Lightcraft Parabolic Reflector showing Ray Tracing for a perfectly focused laser beam.

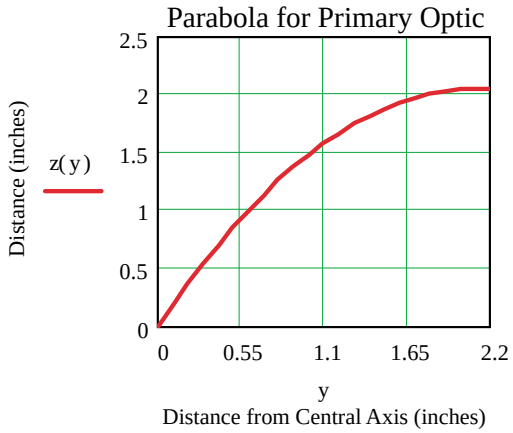

Figure 4.—Plot of Parabola used for Primary Focusing Optic.

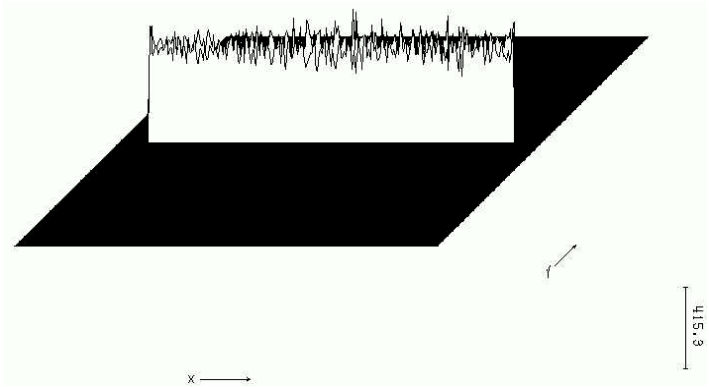

Figure 5.—Laser Intensity in Arbitrary units along upper half, 180°,
of Cowl of the focused laser radiation for Figure 3. Near Constant Intensity.
Spatial Dimensions of Focused Projected Area (Black):
X: 5 inches, Y: 0.25 inches.

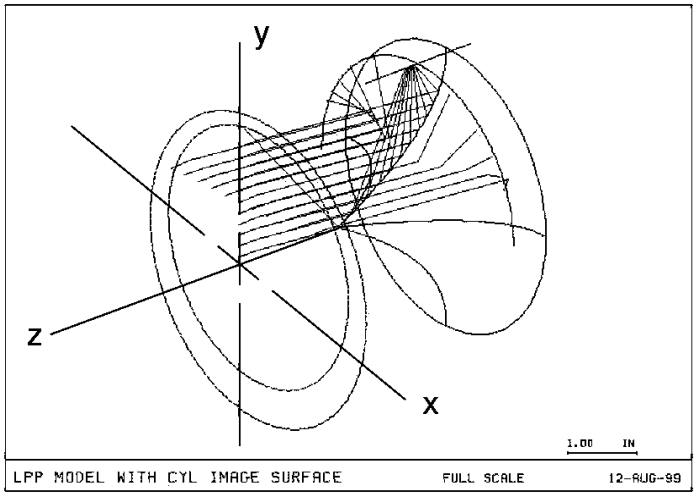

Figure 6.—Code V Optical System of Lightcraft Parabolic Reflector
showing Ray Tracing for a Rotation of 5 degrees about X-axis.

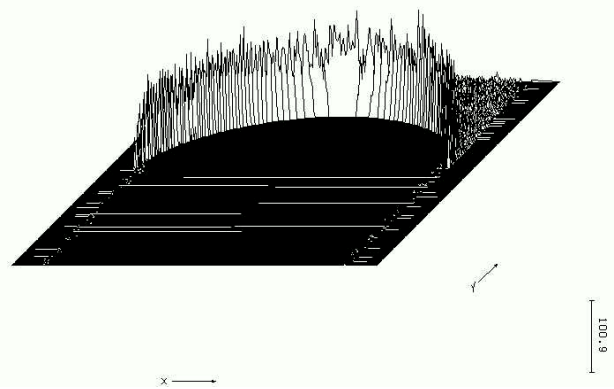

Figure 7.—Five Degree Rotation about the x-axis only. Laser Intensity in arbitrary units of the Focused laser radiation on the Cowl. Near Constant Intensity. Spatial Dimensions: X: 5 inches, Y: 0.25 inches. Peak intensity decreased by a factor of 4.5 from perfectly focused case, well formed ignition line but curved. The intensity is near constant along the arc.

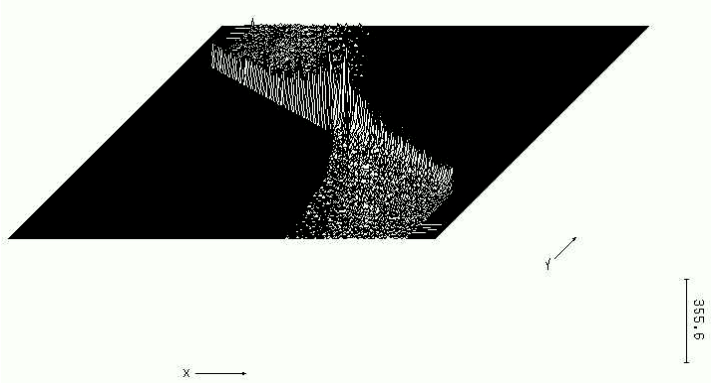

Figure 8.—Five Degree rotation about the y-axis only. Laser Intensity in arbitrary units of the Focused laser radiation on the Cowl. Peak Intensity decreased by a factor of 1.4 in the center from perfectly focused case. Spatial Dimensions: X: 5 inches, Y: 0.25 inches.

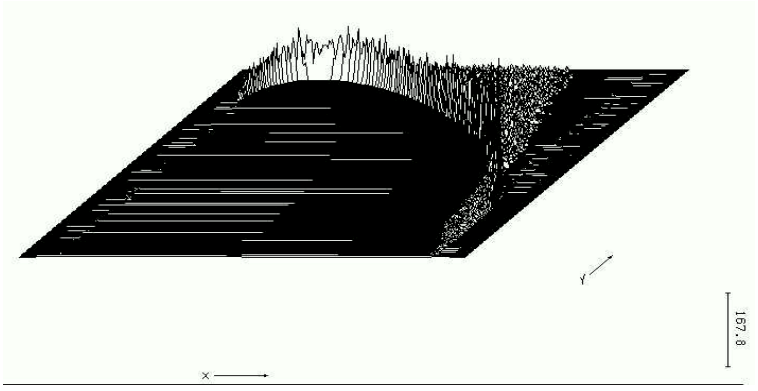

Figure 9.—Five Degree rotation about both the x and y axes. Laser Intensity in arbitrary units of the Focused laser radiation on the Cowl. Peak intensity decreased by a factor of 4.8 from perfectly focused case, well formed ignition line but curved. Spatial Dimensions: X: 5 inches, Y: 0.5 inches.

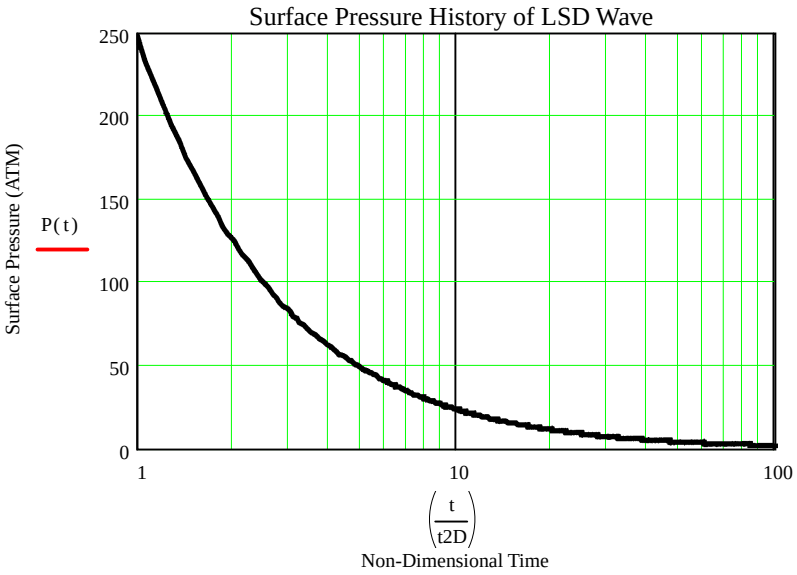

Figure 10.—Surface Pressure History of Blast Wave For Laser Intensity of 5×10^{11} W/m^2.

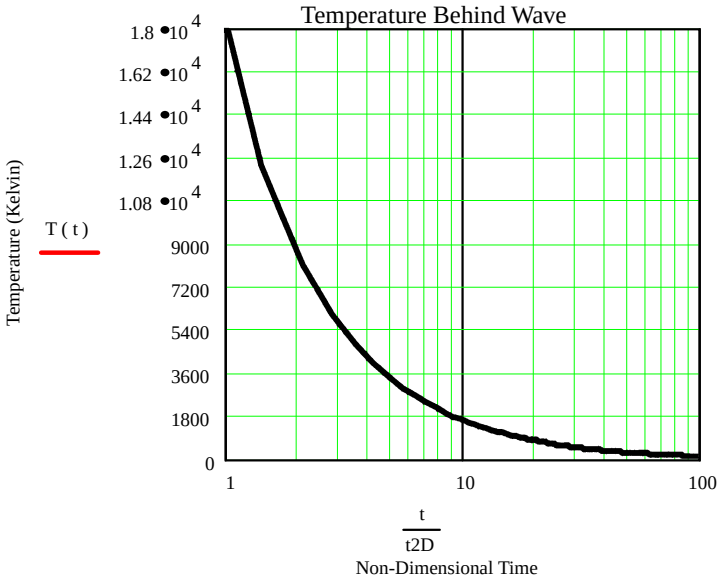

Figure 11.—Equilibrium Temperature behind Shock Wave Decay as a function of time for Laser Intensity of 5×10^{11} W/m^2.

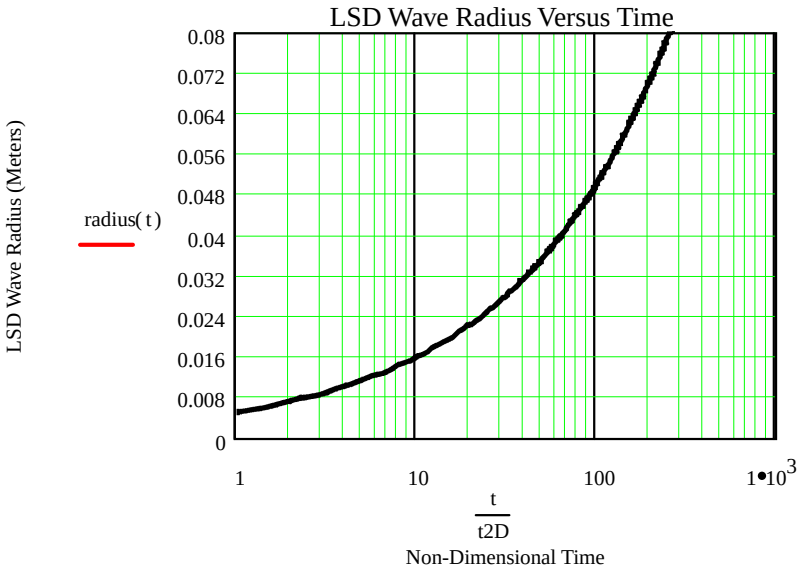

Figure 12.—Shock Wave Radius as a function of time for Laser Intensity of 5×10^{11} W/m^2.

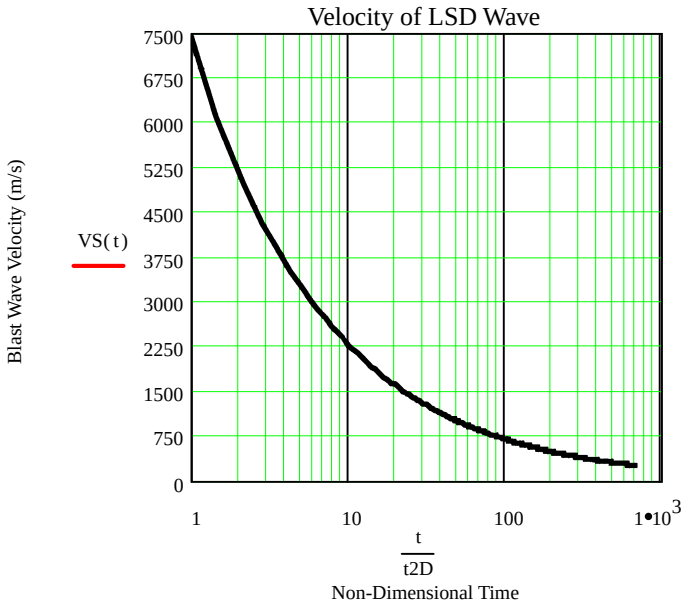

Figure 13.—Shock Wave Velocity as a function of time for Laser Intensity of 5×10^{11} W/m^2.

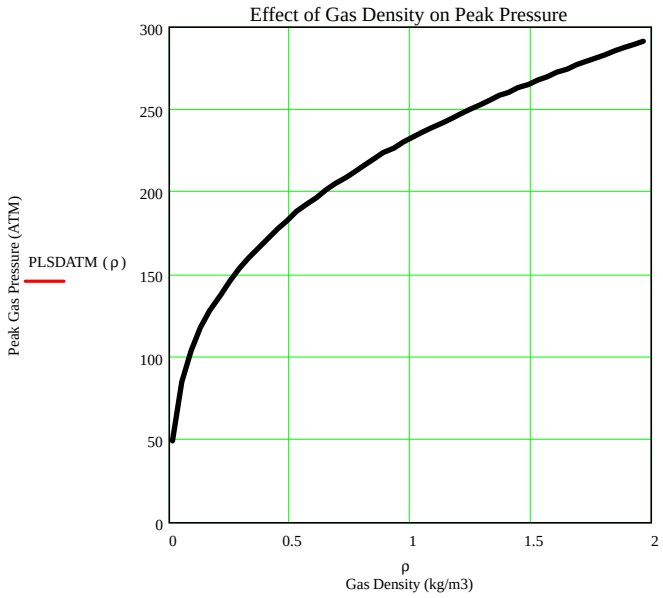

Figure 14.—Effect of Gas Density or Altitude on the Peak Surface Pressure for a Laser Intensity of 5×10^{11} W/m^2.

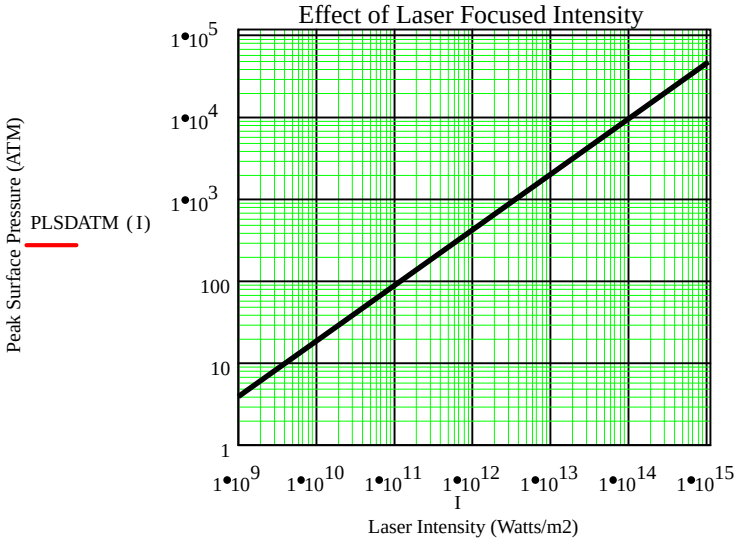

Figure 15.—Effect of Focused Laser Intensity on Peak Surface Pressure, ρ_0 = 1.2 kg/m^3.

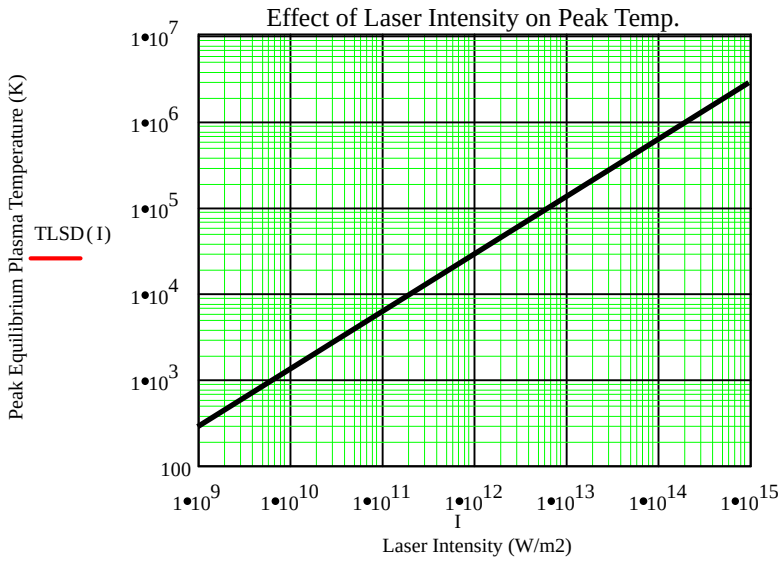

Figure 16.—Effect of Focused Laser Intensity on Peak Equilibrium Gas Temperature, $\rho_0 = 1.2\ kg/m^3$.

REPORT DOCUMENTATION PAGE

Form Approved
OMB No. 0704-0188

1. AGENCY USE ONLY (*Leave blank*)	2. REPORT DATE	3. REPORT TYPE AND DATES COVERED
	June 2000	Technical Memorandum

4. TITLE AND SUBTITLE

Analysis of the Laser Propelled Lightcraft Vehicle

5. FUNDING NUMBERS

WU–101–42–0B–00

6. AUTHOR(S)

Douglas Feikema

7. PERFORMING ORGANIZATION NAME(S) AND ADDRESS(ES)

National Aeronautics and Space Administration
John H. Glenn Research Center at Lewis Field
Cleveland, Ohio 44135–3191

8. PERFORMING ORGANIZATION REPORT NUMBER

E–12359

9. SPONSORING/MONITORING AGENCY NAME(S) AND ADDRESS(ES)

National Aeronautics and Space Administration
Washington, DC 20546–0001

10. SPONSORING/MONITORING AGENCY REPORT NUMBER

NASA TM—2000-210240

11. SUPPLEMENTARY NOTES

Prepared for the 31st Plasmadynamics and Lasers Conference sponsored by the American Institute of Aeronautics and Astronautics, Denver, Colorado, June 19–22, 2000. Responsible person, Douglas Feikema, organization code 6711, (216) 433–5707.

12a. DISTRIBUTION/AVAILABILITY STATEMENT

Unclassified - Unlimited
Subject Categories: 20, 15, and 36 Distribution: Nonstandard

This publication is available from the NASA Center for AeroSpace Information, (301) 621–0390.

12b. DISTRIBUTION CODE

13. ABSTRACT ***(Maximum 200 words)***

Advanced propulsion research and technology require launch and space flight technologies, which can drastically reduce mission costs. Laser propulsion is a concept in which energy of a thrust producing reaction mass is supplied via beamed energy from an off-board power source. A variety of laser/beamed energy concepts were theoretically and experimentally investigated since the early 1970's. During the 1980's the Strategic Defense Initiative (SDI) research lead to the invention of the Laser Lightcraft concept. Based upon the Laser Lightcraft concept, the U.S. Air Force and NASA have jointly set out to develop technologies required for launching small payloads into Low Earth Orbit (LEO) for a cost of $1.0M or $1000/lb to $100/lb. The near term objectives are to demonstrate technologies and capabilities essential for a future earth to orbit launch capability. Laser propulsion offers the advantages of both high thrust and good specific impulse, I_{sp}, in excess of 1000 s. Other advantages are the simplicity and reliability of the engine because of few moving parts, simpler propellant feed system, and high specific impulse. Major limitations of this approach are the laser power available, absorption and distortion of the pulsed laser beam through the atmosphere, and coupling laser power into thrust throughout the flight envelope. The objective of this paper is to assist efforts towards optimizing the performance of the laser engine. In order to accomplish this goal (1) defocusing of the primary optic was investigated using optical ray tracing and (2), time dependent calculations were conducted of the optically induced blast wave to predict pressure and temperature in the vicinity of the cowl. Defocusing of the primary parabolic reflector causes blurring and reduction in the intensity of the laser ignition site on the cowl. However, because of the caustic effect of ray-tracing optics the laser radiation still forms a well-defined ignition line on the cowl. The blast wave calculations show reasonable agreement with previously published calculations and recent detailed CFD computations.

14. SUBJECT TERMS

Propulsion; Future flight

15. NUMBER OF PAGES

20

16. PRICE CODE

A03

17. SECURITY CLASSIFICATION OF REPORT	18. SECURITY CLASSIFICATION OF THIS PAGE	19. SECURITY CLASSIFICATION OF ABSTRACT	20. LIMITATION OF ABSTRACT
Unclassified	Unclassified	Unclassified	